Forbidden transitions in the absorption spectra of C_{60}

K. Yabana [1] and G.F. Bertsch

Department of Physics and Astronomy, Michigan State University, East Lansing, MI 48824, USA
and National Superconducting Cyclotron Laboratory, Michigan State University, East Lansing, MI 48824, USA

Received 8 May 1992; in final form 22 June 1992

Vibrationally induced forbidden transitions in C_{60} are analyzed with a tight-binding Hamiltonian. The predicted electron-vibration coupling is rather weak for low transitions, in agreement with observation. The prominent peaks observed in the 3 eV region are explained as the T_{2u} singlet state coupling to Herzberg–Teller active h_g modes. The vibronic structures observed in the 2 eV region are assigned to singlet $(t_{1u}h_u^{-1})$ states coupled to high frequency h_u and t_{1u} vibrational modes. However, there remains some disagreement with respect to higher energy transitions.

The excitations of the C_{60} microcluster are becoming fairly well characterized through many spectroscopic measurements in the UV, visible, and IR regions [1–7]. There has also been much theoretical work on its electronic structure [8–10] and on its vibrations [9,11,12]. The coupling between the vibrational and electronic degrees of freedom is interesting, as it may play a role in the superconductivity of the alkali-doped solid [13]. In this work, we will calculate the spectroscopic consequences of a model that has been used to investigate the superconductivity. The weak spectroscopic lines seen in the visible spectrum are interesting in this regard, since they arise directly from the vibrational coupling. In this paper we will concentrate on a theoretical analysis of these transitions.

We first review the theoretical spectrum of low-lying electronic excitations. States are characterized by the irreducible representations a, t_1, t_2, g and h of the icosahedral symmetry group. Many theoretical calculations based on the various models predict the lowest particle-hole excited state to be $t_{1u}h_u^{-1}$ configuration and the subsequent excited states to be $t_{1g}h_u^{-1}$ and $t_{1u}h_g^{-1}$ [8–10]. The degeneracy of the particle–hole excited states is partly removed by the electron–electron interaction. Group theoretical analysis leads us to

$$t_{1u}h_u^{-1}: T_{1g}+T_{2g}+G_g+H_g\,,$$

$$t_{1g}h_u^{-1},\ t_{1u}h_g^{-1}: T_{1u}+T_{2u}+G_u+H_u\,. \qquad (1)$$

Among various electronic states, only transitions to $^1T_{1u}$ states are optically allowed from the totally symmetric spin-singlet (^1A_g) ground state of C_{60}. The orbitally forbidden states acquire transition strength through coupling to the molecular vibrations with appropriate symmetry (Herzberg–Teller coupling). The spin-triplet states acquire a small transition strength due to the spin–orbit interaction.

We employ a tight-binding model for the electronic single-particle Hamiltonian

$$h_{sp}=\sum_{\alpha i}\epsilon_\alpha a^\dagger_{\alpha,i}a_{\alpha,i}+\sum_{\alpha\beta ij}t_{\alpha\beta}(r_{ij})a^\dagger_{\alpha,i}a_{\beta,j}\,. \qquad (2)$$

Here i specifies the atom site and $\alpha=$ s, p_x, p_y, p_z specifies the atomic orbital. ϵ_α is the orbital energy and $t_{\alpha\beta}$ are the hopping matrix elements between the different sites, for which we assume r^{-2} dependence. The model is described in more detail in ref. [14] which also gives the parameter values. Application of the model to the electronic excitations is given in ref. [15]. The level ordering and spacing around the Fermi energy are in good agreement with more sophisticated calculations, except that the LUMO–

Correspondence to: K. Yabana, Department of Physics and Astronomy, Michigan State University, East Lansing, MI 48824, USA.

[1] Permanent address: Department of Physics, Niigata University, Niigata 950-21, Japan.

HOMO gap corresponds to the lowest physical excitation rather than the unphysical Hartree–Fock gap.

We first calculate the spectrum of single excitations (particle–hole state) taking the interaction of the form [16]

$$v=\frac{1}{2}\sum_{\alpha\beta ij}\frac{e^2}{|r_i-r_j|+c}\,a^\dagger_{\alpha,i}a^\dagger_{\beta,j}a_{\beta,j}a_{\alpha,i}\,, \tag{3}$$

with $\gamma_{00}=e^2/c=11.1$ eV. In using this interaction, the average of the diagonal exchange matrix elements is subtracted from the calculated energies, since the tight-binding model eq. (2) neglects the difference of the exchange contributions for particle and hole states. We show in fig. 1 the predicted spectrum in the small space composed of the following configurations: $t_{1u}h_u^{-1}$, $t_{1g}h_g^{-1}$, $t_{1g}g_g^{-1}$, $t_{2u}h_u^{-1}$ for even-parity, and $t_{1g}h_u^{-1}$, $t_{1u}h_g^{-1}$, $t_{1u}g_g^{-1}$, $h_gh_u^{-1}$ for odd-parity. The spectrum is quite close to the calculations by other methods [8,9], in particular the number of states below the lowest $^1T_{1u}$ state and their order agree with ref. [9].

Increasing the configuration space to all single excitations will modify the spectrum, effectively screening the electron–electron interaction. The screening also works to suppress the oscillator strength of low-lying allowed transitions, as described in ref. [15]. The effect of the screening would be to compress the spectrum. The screening effect is partly included in our model by the use of the reduced value for the one-center Coulomb integral, $\gamma_{00}=11.1$ eV. At present we do not have enough experimental information regarding the definite strength of the screening effect for the low-lying spectra. However, this present model predicts the lowest triplet state at an excitation energy of 1.6 eV, which is consistent with experiment [17].

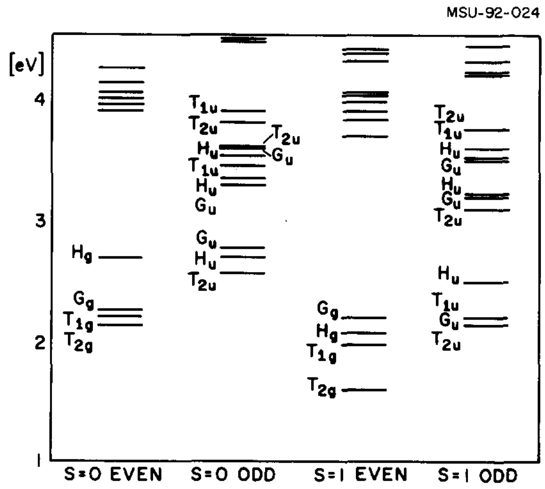

Fig. 1. Electronic energies calculated by the tight-binding model with configuration interaction.

We now briefly discuss the vibrational spectrum. According to the icosahedral symmetry of the C_{60} cluster, there will be 46 non-degenerate vibrational states. Four t_{1u} states have been observed in the infrared absorption spectrum [6,7]. Two a_g and eight h_g states are observed in the Raman scattering experiment [7]. They exhaust the possible modes of the respective symmetries which are expected. We employ the phenomenological spring/mass Hamiltonian of ref. [12] to describe the normal modes of vibration. It describes the low-lying spectra of the molecular vibration fairly well, though it somewhat overestimates the vibrational frequency for the high frequency modes.

We now discuss the electron–vibration coupling. As we will see, the coupling is rather weak and we can use the perturbation theory in which the unperturbed states are constructed from the Hamiltonian at the equilibrium position of the carbon atoms with icosahedral symmetry.

The dipole operator in the tight-binding model is given by

$$D_z=\sum_{\alpha i} z(i)a^\dagger_{\alpha,i}a_{\alpha,i}\,. \tag{4}$$

$z(i)$ is the z component of the ith carbon atom's coordinate. We ignore the dipole transition within the same carbon atom which is not important for the low energy electronic excitation. The dipole operator (4) can directly induce transitions to the forbidden electronic states with vibrational excitation. Let us denote the directional vectors of the normal modes of molecular vibration by $\hat{r}_M$ and the normal coordinates by q_M ($M=1$–174). Expansion of the dipole operator around the equilibrium positions leads us to

$$D_z=\sum_{\alpha i} z_0(i)a^\dagger_{\alpha,i}a_{\alpha,i}$$

$$+\sum_M\left(\sum_{\alpha i} z_M(i)a^\dagger_{\alpha,i}a_{\alpha,i}\right)q_M\,. \tag{5}$$

$z_0(i)$ is the z component of the ith carbon atom's coordinate in the equilibrium position. $z_M(i)$ is the ith carbon atom's z component of $\hat{r}_M$. The second term of eq. (5) can induce directly the vibrational excitation. In numerical calculation, we have found that the transition due to the second term of eq. (5) is much smaller than the transition by way of the Herzberg–Teller coupling which will be discussed next. Therefore we will neglect the second term of eq. (5) in the following discussion.

Next we consider the expansion of the electronic single-particle Hamiltonian (2) about the equilibrium position,

$$h_{\rm sp} = h_{\rm sp}^{(0)} + \sum_M (\hat{r}_M \cdot \nabla h_{\rm sp}) q_M \,. \tag{6}$$

$h_{\rm sp}^{(0)}$ is the electronic single-particle Hamiltonian at the equilibrium. The second term arises from the r_{ij}-dependent hopping matrix elements. ∇ means the derivative with respect to the 180 ($\boldsymbol{r}_i$, $i=1$–60) atomic coordinates.

Only the $^1\mathrm{T}_{1u}$ state can couple to the ground state by the dipole operator. Other forbidded states acquire transition strength through the coupling to the Herzberg–Teller active vibrational modes given in the second term of eq. (6). Let $|\Gamma\alpha\rangle$ represent the electronic state Γ with vibrational excitation of mode α. The dipole transition matrix element between $|\Gamma\alpha\rangle$ and the ground state $|\mathrm{A_g}\rangle$ is given in first-order perturbation theory by

$$\begin{aligned} \langle \Gamma\alpha | D_z | \mathrm{A_g} \rangle = & -\sum_{\mathrm{T_{1u}}} \frac{1}{E_{\mathrm{T_{1u}}} - E_\Gamma - \hbar\omega_\alpha} \\ & \times \langle \Gamma\alpha | H_{\rm coup} | \mathrm{T_{1u}} \rangle \langle \mathrm{T_{1u}} | D_z | \mathrm{A_g} \rangle \\ & - \sum_{\Gamma'} \frac{1}{E_{\Gamma'} + \hbar\omega_\alpha - E_{\mathrm{A_g}}} \\ & \times \langle \Gamma\alpha | D_z | \Gamma'\alpha \rangle \langle \Gamma'\alpha | H_{\rm coup} | \mathrm{A_g} \rangle \,. \end{aligned} \tag{7}$$

The first term comes from the coupling of the state $|\Gamma\alpha\rangle$ to the allowed electronic state $|\mathrm{T_{1u}}\rangle$, and the second term comes from the coupling of the ground state $|\mathrm{A_g}\rangle$ to the excited states, $|\Gamma'\alpha\rangle$. The first term gives the dominant contribution since there is a large energy difference between the ground and excited electronic states in the second term.

The Herzberg–Teller active vibrational modes for the electronic states which appear in (1) are the following

$$\begin{aligned} &\mathrm{T_{1g}}\colon \mathrm{a_u}, \mathrm{t_{1u}}, \mathrm{h_u}\,, && \\ &\mathrm{T_{2g}}\colon \mathrm{g_u}, \mathrm{h_u}, && \mathrm{T_{2u}}\colon \mathrm{g_g}, \mathrm{h_g}\,, \\ &\mathrm{G_g}\colon \mathrm{t_{2u}}, \mathrm{g_u}, \mathrm{h_u}, && \mathrm{G_u}\colon \mathrm{t_{2g}}, \mathrm{g_g}, \mathrm{h_g}\,, \\ &\mathrm{H_g}\colon \mathrm{t_{1u}}, \mathrm{t_{2u}}, \mathrm{g_u}, \mathrm{h_u}, && \mathrm{H_u}\colon \mathrm{t_{1g}}, \mathrm{t_{2g}}, \mathrm{g_g}, \mathrm{h_g}\,. \end{aligned} \tag{8}$$

Since the states appearing in (1) are all degenerate, coupling to the Jahn–Teller active vibrational modes causes further vibrational structure upon each $|\Gamma\alpha\rangle$ state.

In comparing with the empirical spectrum, we shall ignore the triplet states entirely. We have made a calculation of the spin–orbit coupling strength where the matrix elements of orbital angular momentum between different atomic sites are neglected. We have found that the oscillator strength to these spin forbidden states is about a factor 10^{-8} smaller than the strength of the lowest allowed transition. We thus conclude that the spin-triplet states have not been not been observed in the photoabsorption measurements up to the present. The observed weak structures will all be assigned to the vibrationally induced forbidded transitions.

Experimentally, the lowest strong photoabsorption peak is observed at 3.78 eV [1,3,4]. Below it, there are some structures around 3.0 and 2.0 eV regions. Some of the peaks in these regions are very clearly observed [1–4]. Previously, the lowest allowed $^1\mathrm{T}_{1u}$ electronic state was assigned to the 3.0 eV structure [15], but the structure is now well understood as the forbidden electronic state with vibrational excitations. As is seen from fig. 1, the excitation energies of $^1\mathrm{T}_{1u}$ states are pushed up by electron–electron interaction from other forbidden singlet states of odd-parity significantly. Therefore we assign the structures around 3.0 eV to originate from the multiplets $^1\mathrm{T}_{2u}$, $^1\mathrm{G}_u$, and $^1\mathrm{H}_u$. Then the structures at 2.0 eV will be assigned to forbidden electronic states of even-parity dominantly made of the singlet $(\mathrm{t_{1u}h_u^{-1}})$ configuration.

We have made a calculation of the oscillator strength to the forbidden electronic states with Herzberg–Teller active vibrational excitation. We first discuss the spectra in 3 eV region. Fig. 2 shows the oscillator strength for the lowest three odd-parity singlet electronic states, $^1\mathrm{T}_{2u}$, $^1\mathrm{G}_u$ and $^1\mathrm{H}_u$, with vibrational coupling. We assigned three $^1\mathrm{T}_{1u}$ states in

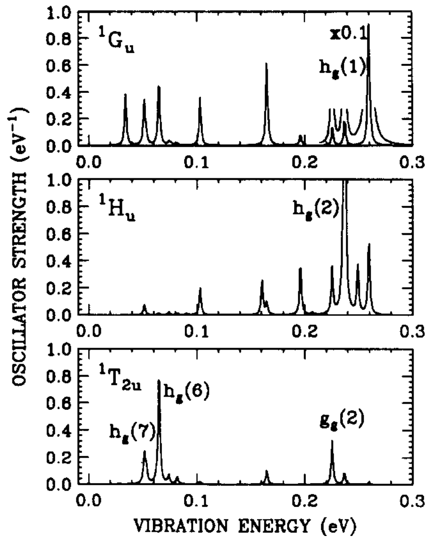

Fig. 2. Oscillator strength for the lowest three odd-parity electronic states with vibrational excitation by Herzberg–Teller coupling. Each level is shown by Lorentzian shape with the width of 0.002 eV.

our calculation to the observed 3.78, 4.84 and 5.88 eV peaks in the photoabsorption measurements [1,3,4]. We set the electronic energies of $^1T_{2u}$, ^1G_u and ^1H_u states to 3 eV.

Two prominent peaks are observed at 398 nm (3.115 eV) and 402.2 nm (3.083 eV) in the R2PI measurement of the molecular beam C_{60} [2]. The same peaks are observed in photoabsorption measurements [1–4] at slightly shifted energies. Nice agreement between our calculation and the observed spectra is seen if we assign them as $h_g(7)$ and $h_g(6)$ vibrations built on the $^1T_{2u}$ state. There are several reasons for this assignment besides apparent agreement of the measured and calculated spectra. As for the assignment of the electronic state, we first note that the $^1T_{2u}$ state is the lowest singlet odd-parity state in the calculated spectra of fig. 1. The same assignment for the electronic state is made in ref. [3] with the magnetic circular dichroism measurement as well as the photoabsorption. For the assignment of the vibrational mode, the energy spacing between two peaks (274 cm^{-1}) is close to the difference of the frequencies of $h_g(7)$ and $h_g(6)$ peaks measured in the Raman scattering (273 cm^{-1} [7]). Furthermore the hot bands corresponding to these peaks are observed in the measurements at room temperature [4,5]. Whetten et al. [5] have suggested from the hot bands analysis the vibrational modes with about 400 and 700 cm^{-1} frequencies are responsible for the 402.4 and 398 nm peaks, respectively. The frequencies of the $h_g(7)$ and $h_g(6)$ modes measured in Raman spectra are 437 and 710 cm^{-1}, respectively [17].

We present a detailed comparison between measured [2] and calculated spectra in the 3 eV region in fig. 3. The calculated oscillator strengths for the $^1T_{2u}$ state with vibrational excitations are plotted at respective excitation energies. We assume that the energy of the electronic state of $^1T_{2u}$ lies at 3.027 eV. The vibrational energies measured by the Raman spectroscopy [7] are used for h_g and a_g modes in plotting the strength, instead of the energies calculated by the spring/mass model. Vibrational energies of g_g states are the estimated values and are more uncertain.

We also included in fig. 3 the progression by the coupling of the totally symmetric and Jahn–Teller active modes to $|^1T_{2u}\alpha\rangle$ states, where α denotes the Herzberg–Teller active vibrational excited state of one quantum. For such a large molecule as C_{60}, the

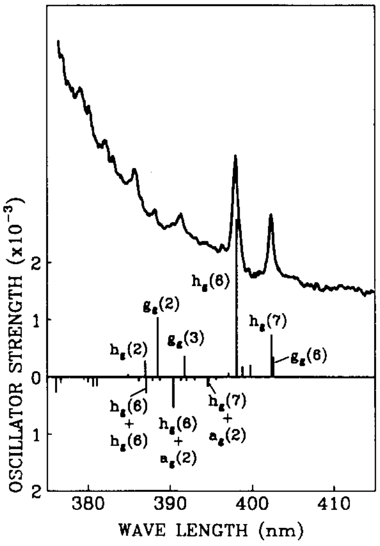

Fig. 3. Calculated oscillator strength for the $^1T_{2u}$ electronic state with vibrational excitations is compared with the measured R2PI spectrum [2]. Upper lines represent the strength for vibrational excitations by Herzberg–Teller coupling, and lower lines represent vibrational excitations with Jahn–Teller as well as Herzberg–Teller coupling.

Jahn–Teller coupling is weak, and perturbation theory may again be employed for the calculation. Jahn–Teller active modes are h_g for T_{1u} states, and g_g and h_g for T_{2u} states. We find that the progressions for a few vibrational modes, for example, $h_g(6)$, $h_g(2)$, $a_g(2)$, and $a_g(1)$, are significant. Their strength is in general less than 20% of the strength of the original state.

Several weak structures above the two prominent peaks at 3.0 eV region are found in the calculated spectra from the Herzberg–Teller coupling to h_g and g_g vibrational modes above $h_g(6)$ and also due to the progression of totally symmetric and Jahn–Teller active vibrational modes. Refined data are needed to make a detailed assignment. Below 385 nm, contribution from the other electronic states, ^1G_u and ^1H_u, with vibrational excitations seems to be necessary to explain the spectra.

The relative oscillator strength summed over the peaks of the 3 eV region are presented in ref. [3] to be 0.013, relative to the strength of lowest allowed transition at 3.78 eV. The calculated strength for $^1T_{2u}$ with vibrational excitations is 0.0055. Thus the calculated vibrational coupling is somewhat too weak, although part of the strength could be due to contributions from ^1G_u and ^1H_u electronic states in the 3 eV region.

Though the calculated results are quite convincing for the $^1T_{2u}$ state, there remains a disagreement. Our calculation predicts prominent structures for ^1H_u and ^1G_u states, too. Among them, the oscillator strength for the ^1G_u state with $h_g(1)$ vibrational excitation is about an order of magnitude larger than that of $^1T_{2u}$ with $h_g(6)$ vibration which we assigned as the 398 nm peak. Experimentally, no such strong peak has been observed [3–5].

Let us turn to the region around 2.0 eV. Our assignment for the structures in this energy region is the electronic states composed of $(t_{1u}h_u^{-1})$. We made a calculation of the oscillator strength assuming the lowest four singlet even-parity states in fig. 1 to lie at 2 eV. Results are shown in fig. 4. For each state, relatively strong features are seen in the states with high-lying frequency vibrational modes of h_u, g_u and t_{1u} symmetry. We therefore expect prominent peaks in the 2 eV region in the photoabsorption spectra accompany the vibrational modes with high frequency. Calculation of the electronic spectra in fig. 1 shows that the three electronic states, $^1T_{2g}$, $^1T_{1g}$ and ^1G_g, are nearly degenerate within 0.1 eV. The vibrational structures upon them are thought to be responsible for the structures at the 2 eV region, overlapping each other. At present, it seems difficult to present detailed assignment for the structures in this energy region.

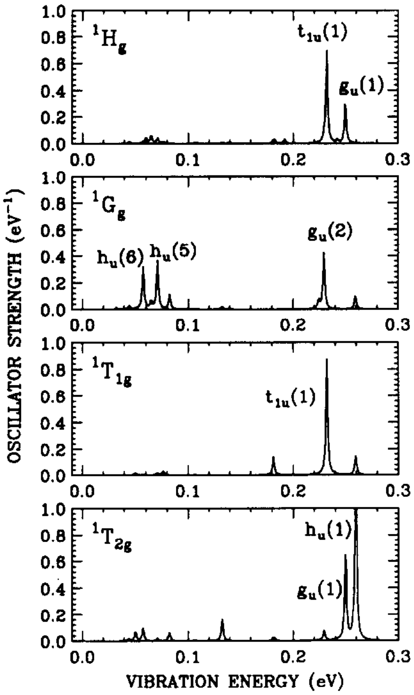

Fig. 4. Oscillator strength for the lowest four even-parity electronic states with vibrational excitations by Herzberg–Teller coupling.

The oscillator strength summed over four structures relative to the lowest allowed peak is measured in ref. [3] to be 0.0025. The calculated relative oscillator strength for $^1T_{2g}$ states with vibrational excitation, which include two prominent peaks, is 0.0076. The calculated oscillator strength summed over three electronic states, $^1T_{2g}$, $^1T_{1g}$ and ^1G_u, which are almost degenerate in fig. 1, is 0.0156. Thus the calculation somewhat overestimates the observed strength.

In summary, we have applied the tight-binding Hamiltonian to vibrationally induced forbidded transitions. The two prominent peaks observed in the photoabsorption at about 3.0 eV are assigned to the $^1T_{2u}$ electronic states with $h_g(7)$ and $h_g(6)$ vibrational excitation, and the observed coupling strength is well accounted for by the model. The structures around 2.0 eV are expected to consist of the singlet electronic states composed of $(t_{1u}h_u^{-1})$ LUMO–HOMO configuration coupled to the rather stiff h_u, g_u and t_{1u} vibrational modes. One final note: the vibrational coupling is rather weak and incapable of explaining the widths of the allowed transitions at 3.78, 4.84 and 5.88 eV.

We thank D. Nocera for conversations. One of the authors (KY) is indebted to the Nishina Memorial Foundation for financial support for his stay in Michigan State University. This work was supported by NSF grant 89-20927.

References

[1] J.R. Heath, R.F. Curl and R.E. Smalley, J. Chem. Phys. 87 (1987) 4236;
H. Ajie, M.M. Alvarez, S.J. Anz, R.D. Beck, F. Diederich, K. Fostiropoulos, D.R. Huffman, W. Krätschmer, Y. Rubin, K.E. Schriver, D. Sensharma and R.L. Whetten, J. Phys. Chem. 94 (1990) 8630;
J.P. Hare, H.W. Kroto and R. Taylor, Chem. Phys. Letters 177 (1991) 394;
C. Reber, L. Yee, J. McKiernan, J.I. Zink, R.S. Williams, W.M. Tong, D.A.A. Ohlberg, R.L. Whetten and F. Diederich, J. Phys. Chem. 95 (1991) 2127.

[2] R.E. Haufler, Y. Chai, L.P.F. Chibante, M.R. Fraelich, R.B. Weisman, R.F. Curl and R.E. Smalley, J. Chem. Phys. 95 (1991) 2197.

[3] Z. Gasyna, P.N. Schatz, J.P. Hare, T.J. Dennis, H.W. Kroto, R. Taylor and D.R.M. Walton, Chem. Phys. Letters 183 (1991) 283.

[4] S. Leach, M. Vervloet, A. Despres, E. Breheret, J.P. Hare, T.J. Dennis, H.W. Kroto, R. Taylor and D.R.M. Walton, preprint (1991).

[5] R.L. Whetten, M.M. Alvarez, S.J. Anz, K.E. Schriver, R.D. Beck, F.N. Diederich, Y. Rubin, R. Ettl, C.S. Foote, A.P. Darmanyan and J.W. Arbogast, Mat. Res. Soc. Symp. Proc. 206 (1991) 639.

[6] W. Krätschmer, K. Fostiropoulos and D.R. Huffman, Chem. Phys. Letters 170 (1990) 167.

[7] D.S. Bethune, G. Meijer, W.C. Tang, H.J. Rosen, W.G. Golden, H. Seki, C.A. Brown and M.S. de Vries, Chem. Phys. Letters 179 (1991) 181.

[8] I. Laszlo and L. Udvardi, J. Mol. Struct. 183 (1989) 271; Chem. Phys. Letters 136 (1987) 418.

[9] F. Negri, G. Orlandi and F. Zerbetto, Chem. Phys. Letters 144 (1988) 31.

[10] J. Feng, J. Li, Z. Wang and M.C. Zerner, Intern. J. Quantum Chem. 37 (1990) 599;
S. Larsson, A. Volosov and A. Rosen, Chem. Phys. Letters 137 (1987) 501;
P.W. Fowler, P. Lazzeretti and R. Zanasi, Chem. Phys. Letters 165 (1990) 79;
S. Satpathy, Chem. Phys. Letters 130 (1986) 545;
R.C. Haddon, L.E. Brus and K. Raghavachari, Chem. Phys. Letters 125 (1986) 459;
M. Braga, S. Larsson, A. Rosen and A. Volosov, Astron. Astrophys. 245 (1991) 232.

[11] R.E. Stanton and M.D. Newton, J. Phys. Chem. 92 (1988) 2141.

[12] D.E. Weeks and W.G. Harter, Chem. Phys. Letters 144 (1988) 366.

[13] M. Lannoo, G.A. Baraff, M. Schlülter and D. Tomanek, Phys. Rev. B 44 (1991) 12106.

[14] D. Tomanek and M.A. Schlutter, Phys. Rev. Letters 67 (1991) 2331.

[15] G.F. Bertsch, A. Bulgac, D. Tomanek and Y. Wang, Phys. Rev. Letters 67 (1991) 2690.

[16] N. Mataga and K. Nishimoto, Z. Physik. Chem. (Frankfurt) 12 (1957) 335; 13 (1957) 140.

[17] J.W. Arbogast, A.P. Darmanyan, C.S. Foote, Y. Rubin, F.N. Diederich, M.M. Alvarez, S.J. Anz and R.L. Whetten, J. Phys. Chem. 95 (1991) 11;
M. Terazima, N. Hirota, H. Shinohara and Y. Saito, J. Phys. Chem. 95 (1991) 9080.